Brain Research Bulletin 144 (2019) 75–84

Contents lists available at ScienceDirect

Brain Research Bulletin

journal homepage: www.elsevier.com/locate/brainresbull

Research report

Entorhinal cortex stimulation induces dentate gyrus neurogenesis through insulin receptor signaling

Abdolaziz Ronaghi[a], Mohammad Ismail Zibaii[b], Sareh Pandamooz[a], Nasrin Nourzei[a], Fereshteh Motamedi[a], Abolhassan Ahmadiani[a], Leila Dargahi[c,*]

[a] Neuroscience Research Center, School of Medicine, Shahid Beheshti University of Medical Sciences, Tehran, Iran
[b] Laser and Plasma Research Institute, Shahid Beheshti University, Tehran, Iran
[c] Neurobiology Research Center, Shahid Beheshti University of Medical Sciences, Tehran, Iran

ARTICLE INFO

Keywords:
Deep brain stimulation
Entorhinal cortex
Neurogenesis
Insulin receptor

ABSTRACT

Deep brain stimulation (DBS) has been established as a therapeutically effective method to treat pharmacological resistant neurological disorders. The molecular and cellular mechanisms underlying the beneficial effects of DBS on the brain are not yet fully understood. Beside numerous suggested mechanisms, regulation of neurogenesis is an attractive mechanism through which DBS can affect the cognitive functions. Considering the high expression of insulin receptors in hippocampus and also impaired neurogenesis in diabetic brain, the present study aimed to examine the role of insulin receptor signaling in DBS induced neurogenesis. High frequency stimulation was applied on the entorhinal cortex of rats and then neurogenesis markers in the dentate gyrus region of the hippocampus were examined using molecular and histological methods in the sham, DBS and insulin receptor antagonist-treated groups. In parallel, the changes in insulin receptor signaling in the hippocampus and spatial learning and memory performance were also assessed. DBS promoted adult hippocampal neurogenesis and facilitated the spatial memory concomitant with changes in insulin receptor signaling parameters including IR, IRS2 and GSK3β. Application of insulin receptor antagonist attenuated the DBS-induced neurogenesis. Our data emphasize that entorhinal cortex stimulation promotes adult hippocampal neurogenesis and facilitates spatial learning and memory at least partly through insulin receptors. Notably, GSK3β inhibition can play a major role in the downstream of insulin receptor signaling in DBS induced neurogenesis.

1. Introduction

Currently, deep brain stimulation (DBS) has been established as a therapeutic method for the treatment of movement disorders more specifically Parkinson's disease with poor response to pharmacological manipulations (Deuschl et al., 2006). DBS has also been suggested as a new therapeutic approach for the treatment of disorders of mood and cognition (Laxton et al., 2010; Stone et al., 2011) and to alleviate dependency in addiction behaviors (Creed et al., 2015). However, in spite of the progressive application of DBS in neurodegenerative and neurogenic disorders, detailed mechanisms mediating these clinical effects remain largely unknown. Many lines of mechanisms have been suggested for the pro-cognitive effect of DBS. For example, DBS can modulate the neural circuit of target regions (Mayberg et al., 2005), modulate neurotransmitter release in neuron level (Kringelbach et al., 2007) or restore basal activity within the dysregulated brain region (Chiken and Nambu, 2016). According to accumulating data, the most remarkable suggested potential mechanism through which DBS may improve cognitive functions is activity-dependent regulation of hippocampal neurogenesis (Encinas et al., 2011; Stone et al., 2011).

Neurogenesis as a basic phenomenon adds new neurons to some specific well-known regions of the brain such as the sub-granular zone (SGZ) of the dentate gyrus (DG) in the adult mammalian hippocampus, which plays an essential role in memory formation (Ming and Song, 2005; Zhao et al., 2008). While the hippocampus and DG receive many projections from many regions of the brain, the entorhinal cortex (EC) provides the main afferent input to the DG (Andersen et al., 2007). It has been shown that stimulation of specific targets that project into the hippocampus in rodents, e.g., the anterior thalamic nucleus (Encinas et al., 2011) and EC/perforant path (Kitamura et al., 2010; Stone et al., 2011), promotes the proliferation and differentiation of neural precursor cells and/or survival of adult-generated neurons. However, the underlying molecular mechanisms and neurotransmitters/modulators involved are not well known.

* Corresponding author.
E-mail address: l.dargahi@sbmu.ac.ir (L. Dargahi).

https://doi.org/10.1016/j.brainresbull.2018.11.011
Received 9 October 2018; Received in revised form 14 November 2018; Accepted 20 November 2018
Available online 22 November 2018

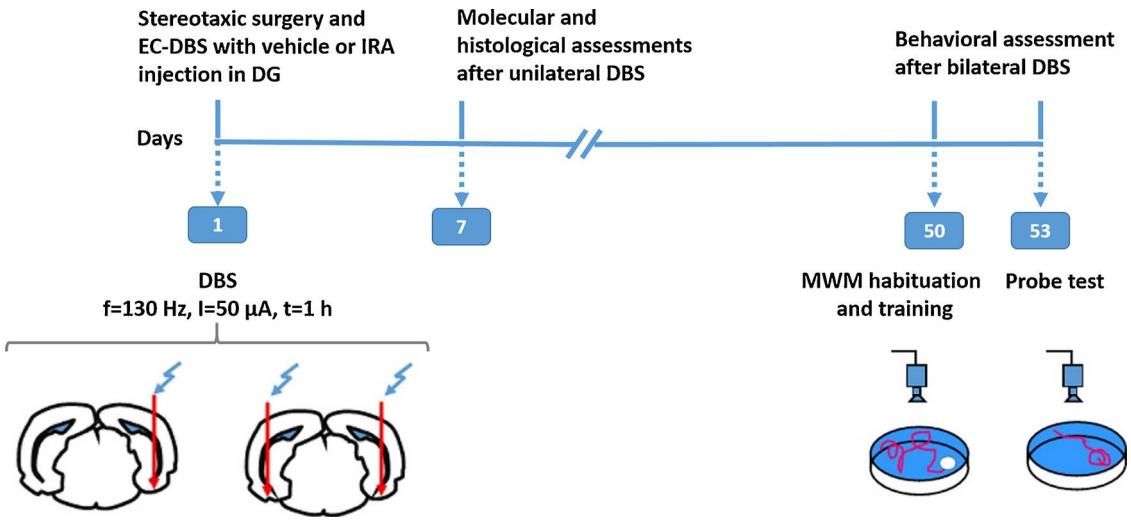

Fig. 1. Schematic illustration of the experimental time line. DBS, deep brain stimulation; EC, entorhinal cortex; IRA, insulin receptor antagonist; DG, dentate gyrus.

Neuromodulation via insulin signaling has recently gained attention in different health and disease conditions. Insulin receptors (IRs) have been found in many regions of the brain, especially with high density in the hippocampal formation (W.-Q. Zhao and Alkon, 2001). Insulin binding to the IR leads to autophosphorylation of the receptor which initiates several signaling cascades. PI3K/Akt/GSK-3β, which is one of the well-known pathways of IR signal transduction in the brain, has been shown to be implicated in neurogenesis (Zheng et al., 2017) and learning and memory functions (van der Heide et al., 2006; Zhao et al., 2004). Autophosphorylation of the IR is followed by tyrosine phosphorylation of the insulin receptor substrate (IRS) protein family. Phosphorylated IRS binds to several effector molecules such as p85 or p55 regulatory subunit of phosphatidylinositol 3-kinase (PI3K), and triggers activation of PI3K, which in turn phosphorylates and activates protein kinase B/Akt. Akt phosphorylates glycogen synthase kinase 3β (GSK-3β) at the serine 9 residues and inactivates it (Perluigi et al., 2014). Another ligand for the IRs is insulin-like growth factor 1 (IGF-1) which besides its own receptor, can bind to IRs and initiate the same signaling pathways (Boura-Halfon and Zick, 2009). The involvement of insulin signaling in neural stem cell proliferation, differentiation and homeostasis has been shown in some in vitro studies (Gutiérrez et al., 2007; Yu et al., 2008; Ziegler et al., 2015). On the other hand, impaired neurogenesis is reported in the diabetic mouse and rat brains (Noor and Zahid, 2017; Mishra et al., 2018). However, there is no clear study on the role of insulin signaling in activity dependent neural proliferation and differentiation in adult wild-type brain in the literature.

With this background, in this study, we used DBS as an approach to stimulate the medial EC with a localized targeting precision. Neurogenesis in the dentate gyrus in parallel to changes in insulin receptor signaling pathway was assessed through molecular, histological and behavioral analyses. The role of insulin receptors was also studied using insulin receptor antagonist.

2. Materials and methods

2.1. Animals

Adult male Wistar rats weighing 250–270 g at the beginning of the experiments, were used in this study. Animals were housed in groups of four per cage with free access to water and food under the controlled laboratory conditions (12 h light/dark cycle with a constant temperature of 21 ± 2 °C). All experimental procedures were approved by the Ethics Committee of Shahid Beheshti University of Medical Sciences (IR.SBMU.SM.REC.1394.147) in accordance with the international guidelines by the National Institutes of Health (No. 80-23, revised 1996).

2.2. Stereotaxic surgery, electrical stimulation and drug delivery

Rats were anesthetized with chloral hydrate (400 mg/kg, i.p.), and placed in a stereotactic frame. The scalp was incised and skull hole(s) with coordinates relative to the bregma in the anteroposterior (AP), mediolateral (ML), and dorsoventral (DV) planes were drilled as follows (in mm): (1) EC [AP = -6.84, ML= ± 4.8, DV = 8.8] for the stimulating electrode and, (2) DG [AP = -3.84, ML = ± 2.3, DV = 3.3] (Paxinos and Watson, 2007) for drug delivery. Vehicle (normal saline) or insulin receptor antagonist (IRA: S961, Phoenix Pharmaceuticals, Inc, 0.5 nmol in 2 µl normal saline) was administered using a Hamilton syringe 30 min before the DBS or sham operation. Brain electrical stimulation was delivered via a bipolar stainless steel electrode (0.125 mm diameter, Advent, UK), in which the tips were about 0.5 mm apart. Stimulation was applied with a stimulus isolator (A365R, WPI, Sarasota FL, USA) with the frequency of 130 Hz, pulse width of 90 µs (square wave), 50 µA current and duration of 60 min. This high-frequency DBS was chosen according to that usually used in the clinical practice (Volkmann et al., 2006). Laterality (unilateral or bilateral) of stimulation varied by experiment. Schematic design of the experimental timeline and protocol was shown in Fig. 1.

2.3. RNA extraction, cDNA synthesis and quantitative polymerase chain reaction (qPCR)

Seven days after unilateral sham operation or DBS, three to five rats per sham, DBS and IRA + DBS groups were sacrificed and total RNA was extracted from the hippocampus using YTzol reagent according to the manufacturer's protocol (Yekta Tajhiz Azma, Tehran, Iran). The sham operation group served as the control which animals were operated, inserted electrode and received vehicle without stimulation. The RNA quality was evaluated by determining 18S and 28S ribosomal RNA bands using electrophoresis, and the ratio of absorbance at 260/280 nm. Then 2 µg of total RNA was reverse transcribed to cDNA using TransScript First-Strand cDNA Synthesis Kit (Yekta Tajhiz Azma, Tehran, Iran) according to the manufacturer's instructions. Briefly, RNA template, primer, and DEPC-treated water were mixed and incubated at 70 °C for 5 min and chilled on ice. In the next step the prepared mixture of 5x first-strand buffer 4 µl, dNTPs (10 mM) 1 µl, RNasin (40U/µl) 0.5 µl and M-MLV (200U/µl) 1 µl was added to the step one solution and then incubated for 60 min at 42 °C. The reaction was terminated by

Table 1
Primer sequences used for qPCR.

Gene	Forward primer (5'-3')	Reverse primer (5'-3')
Nestin	GGAGCAGGAGAAGCAAGGTC	GAGTTCTCAGCCTCCAGCAG
DCX	GGAAGGGGAAAGCTATGTCTG	TTGCTGCTAGCCAAGGACTG
IR	GAGCGGAGGAGTCTTCATT	GGTGTAGTGGCTGTCACATT
IRS2	GACTTCTTGTCCCATCACTTGAAA	GCTAAGCATCTCCTCAGAATGGA
β- actin	TCTATCCTGGCCTCACTGTC	AACGCAGCTCAGTAACACTCC

heating at 70 °C for 5 min. The resulting cDNA was then used for quantitative measurement of genes expression using SYBR Green Real-Time PCR Master Mix (Ampliqon) reagents and ABI System by the following cycling conditions; activation 10 min at 95 °C, denaturation 15 s at 95 °C, annealing 30 s at optimum temperature, extension 30 s at 72 °C. The threshold cycles (Ct) were used to quantify the mRNA levels of the target genes. We used the $2^{-\Delta\Delta Ct}$ method (Xu et al., 2014) to calculate the relative gene expression, normalized to the β-actin housekeeping gene and relative to the control group. Primers sequences have been listed in Table 1.

2.4. Western blotting

To investigate the hippocampal insulin receptor signaling changes after the unilateral DBS, three to five rats per sham, DBS and IRA + DBS groups were sacrificed at day seven post-surgery. The brain was rapidly removed and the hippocampus was dissected on ice and stored at −80 °C until the western blot analysis. Total tissue was homogenized in the lysis buffer [50 mM Tris−HCl, pH 8.0, 150 mM NaCl, 0.1% Triton X-100, 0.25% sodium deoxycholate, 0.1% sodium dodecyl sulfate (SDS), 1 mM EDTA, 1 mM Sodium orthovanadate, 15 mM Sodium pyrophosphate, 50 mM Sodium fluride and 1 mM PMSF]. Protein concentration was determined using the BCA method (BCA Protein Assay Kit, Thermo Scientific, USA) and protein samples (60 µg) were loaded on the electrophoresis gel. Samples were separated by electrophoresis on 12% SDS-PAGE, transferred to a polyvinylidene difluoride (PVDF) membrane (Millipore, Billercia, MA) and blocked with 2% non-fat dry milk (Amersham, ECL Advance TM) for 1 h at room temperature. Afterwards, the blots were probed with anti-Akt1/2/3 (H-136) antibody (1:1000; Santa Cruz, sc-8312), anti-p-Akt1/2/3 (Ser473) antibody (1:1000; Santa Cruz, sc-101629), anti-GSK3β (27C10) antibody (1:1000; Cell Signaling, 9315), anti-Phospho-GSK3β (Ser9) antibody (1:1000; Cell Signaling, 9323) overnight at 4 °C. Next day, the blots were washed and incubated with HRP-conjugated Goat Anti-Rabbit IgG H&L (HRP) antibody (1:12000, Abcam, ab6721) for 1 h at room temperature. Subsequent visualization was performed using an enhanced chemiluminescence system (ECL, BIO RAD, USA). β-Actin expression was analyzed using anti β-Actin (13E5) rabbit monoclonal antibody (1:750; Cell signaling, 4970) as an internal control for normalization of protein amounts. Finally, results were quantified by the scan of X-ray films and analysis by Image *J* software.

2.5. Immunohistochemistry

In this study, seven days after the DBS or sham operation, transcardial perfusion of rats with 0.1 M PBS and 4% paraformaldehyde (PFA) was performed and, the removed brains were postfixed in PFA overnight and then were immersed in 30% sucrose (Merck, Germany) for 2 days at 4 °C and finally embedded in OCT (optimum cutting temperature) solution (Sakura, Japan). The immunostaining was carried out on the 20-micrometer coronal sections of cryopreserved brains. Sections localized to the 3.4–3.9 mm posterior to the bregma (Paxinos and Watson, 2007) were used for staining. At least three rats per group and three sections per rat were included in the study. Sections were fixed with acetone (Merck, Germany) for 20 min, then were quenched in the 1% hydrogen peroxide (Merck, Germany) and permeabilized in the 0.2% Triton X-100 (Merck, Germany).The 10% goat serum (Sigma, USA, prepared in 0.2% Triton X-100) was used for blocking, and primary antibody was employed after dilution in blocking buffer and incubated overnight at 4 °C. The following primary antibodies were used: rabbit anti-Doublecortin (DCX) (1:200, Abcam, ab77450), rabbit anti-Nestin (1:100, Abcam, ab93157), rabbit- anti Ki67 (1:100, Abcam, ab66155). In addition, goat anti-rabbit IgG FITC conjugated (1:100, Sigma, F1262) was employed on the second day of staining and the cells' nuclei were counterstained with DAPI (Sigma). Stained sections were visualized and imaged by fluorescent microscopy Nikon E600 equipped with DS-Ri2 camera, at ×200 magnification.

2.6. Morris water maze (MWM) protocol

Fifty days after bilateral DBS or sham operation, six rats per group were subjected to spatial learning and memory test. The water maze was consisted of a black circular pool (150 cm in diameter, 60 cm high, and 45 cm depth) filled with water around 23°c (Fig. 4A). A black circular escape platform (11 cm diameter) was submerged about 2 cm under the water surface. It was positioned in the center of one arbitrarily designed quadrant. The room was decorated with dark curtain and some distinct pictures in the fixed position during the experiment that served as spatial cues on the walls. A CCD camera (Panasonic Inc., Japan) was mounted above the maze and recorded rat's locomotion. The camera was connected to a computer which was equipped with the Ethovision software (version XT7, Netherlands). Animals were trained with undertraining protocol over 3 days with three trials per day (inter-trial interval, 30 s). On each trial, rats were released into the pool, facing the wall, in one of four defined quadrants (the order of each trial was detected randomly throughout training). Rats were given 60 s to swim and find the platform. The trial was accomplished once the rats found the platform and stayed there for 20 s, or 60 s had elapsed that in this case rats were guided to the platform by the experimenter. Latency to find the platform and distance moved to find the platform were recorded in the training sessions. Qualitative aspects of learning the water maze task were also analyzed during training trials (Garthe, et al., 2009; Stone et al., 2011). Briefly, swim path data from Ethovision (Noldus, NL) were used for classifying the respective predominant search strategies by visual analysis by an experimenter. Trial tracks were classified as direct swim, focal search, directed search, chaining, scanning, random search, perseverance and thigmotaxis as defined in Fig. 5B, adapted form Stone et al. (2011) and Garthe et al. (2009).

One hour after the last training trial, as the probe session for spatial memory assessment, the platform was removed and the trained animals released to the water from the opposite quadrant of the platform site for the 60 s in a series of three tests with an inter-test interval of 3 min. The time spent in the target quadrant, the number of crossings the platform location and latency to first cross the removed platform were recorded in the probe sessions.

2.7. Statistical analysis

In the molecular studies, data analysis was performed by two-way ANOVA, and Bonferroni multiple range tests were used for post hoc analyses of significant main effects. Behavioral data in training parameters was analyzed using repeated measure two-way ANOVA. Swim strategy frequencies were compared during trials within groups using nonparametric Friedman's test. Parameters in the probe session were analyzed by using one-way ANOVA followed by Tukey post-test. GraphPad Prism Software (version 6) was used to carry all statistical analyses. *P* value less than 0.05 was considered statistically significant.

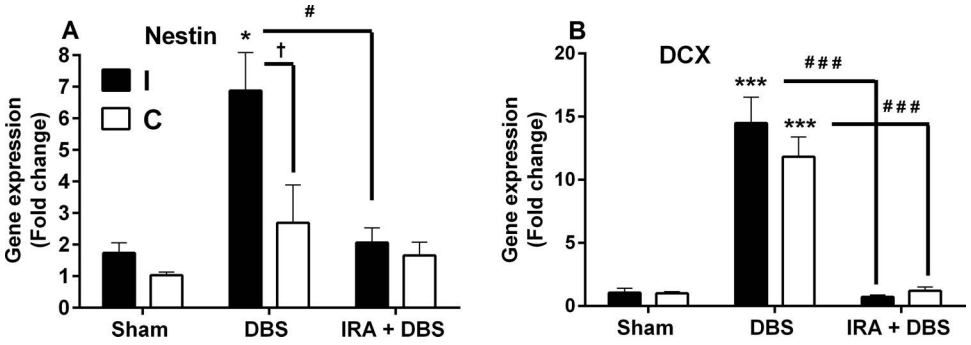

Fig. 2. The effect of unilateral entorhinal cortex stimulation on mRNA expression of neurogenesis markers in hippocampus. The qPCR data analysis of Nestin shows an obvious increase in mRNA level of this marker in the ipsilateral *(I)* side of the DBS group and attenuation in the IRA + DBS group **(A)**. The qPCR data analysis of DCX shows an obvious increase in mRNA level of this marker in the both ipsilateral *(I)* and contralateral *(C)* sides of the DBS group and then attenuation in the IRA + DBS group **(B)**. Data represent Mean ± SEM. n = 3-5. $^{*}p < 0.05$ and $^{***}p < 0.001$ vs. corresponding sham group. $^{\#}p < 0.05$ and $^{\#\#\#}p < 0.001$ vs. DBS group. $^{\dagger}p < 0.05$ between two sides in the DBS group. DBS, deep brain stimulation; DCX, doublecortin; IRA, insulin receptor antagonist.

3. Results

3.1. IRA attenuated the increase of neurogenesis markers in response to EC stimulation

Seven days after unilateral EC stimulation, DG cell proliferation and neurogenesis markers were evaluated at the level of mRNA and protein. Day 7 post stimulation was selected as an optimum time point to track the initiation of neurogenesis process in SGZ (Kee et al., 2007; Kempermann et al., 2015).

In qPCR test, two-way ANOVA analysis revealed that mRNA of Nestin, the well-known neuroprogenitor marker, has been changed significantly in the hippocampus of animals between the treated groups [treatment main effect: $F_{(2, 14)} = 9.14$, $P = 0.003$; side (ipsilateral and contralateral) main effect: $F_{(1, 14)} = 5.47$, $P = 0.034$]. Further Bonferroni post-test analysis showed a significant increase in the mRNA level of Nestin in the ipsilateral side to the stimulation site in the DBS group in comparison with the corresponding side of the sham group and also to the contralateral side to the DBS ($P < 0.05$). This elevation was abolished in the IRA + DBS group ($P < 0.05$) (Fig. 2A).

On the other hand, the level of DCX, known as a neuroblast marker significantly changed in different treated groups [treatment main effect: $F_{(2, 12)} = 84.7$, $P = 0.0001$]. Bonferroni post-test analysis showed the significant elevation in mRNA level in the DBS group in both ipsilateral and contralateral sides in comparison with the corresponding sides in the sham group ($P < 0.001$). The DBS-induced DCX mRNA transcription were attenuated in the IRA + DBS group ($P < 0.001$) (Fig. 2B).

In the immunohistochemical analysis as shown in Fig. 3A, expression of Ki67, as a proliferation marker, in the stimulated animals was greater than the non-stimulated sham group in ipsilateral to electrode site. In addition, ectopic Ki67 positive cells also were seen in the hilus region. Interestingly, this elevation was abolished in the IRA + DBS group. Nestin expression also followed a same pattern as shown in Fig. 3B. The expression of this protein was elevated in the DBS group compared with the sham group. However, in the IRA + DBS group, comparable elevation of Nestin expression was not observed. In Fig. 3C, different level of DCX expression in the DG region of animals in all groups has been shown in both sides. Images have shown elevated expression of DCX in the DBS group especially in the stimulated side with ectopic migration, in comparison to the sham group, and this elevation of expression was attenuated in the IRA + DBS group.

3.2. Entorhinal cortex stimulation affected IR signaling in the hippocampus

After showing the effect of EC stimulation on the promotion of DG neurogenesis, to examine the effects of EC-DBS on insulin signaling pathway molecules (IR/IRS2 /Akt/GSK3β), we used qPCR and western blot analysis. Two-way ANOVA revealed a significant change in the mRNA level of IR between groups and brain hemispheres [treatment main effect: $F_{(2, 12)} = 5.183$, $P = 0.023$; side main effect: $F_{(1, 12)} = 5.712$, $P = 0.0341$]. Bonferroni post-test showed a significant increase in the mRNA level of IR in the ipsilateral side of the DBS group ($P < 0.05$). However blocking IR receptors by IRA before the DBS, inhibited this increase ($P < 0.05$) (Fig. 4A). The insulin receptor substrate 2, IRS2, showed the similar results using qPCR technique [treatment main effect; $F_{(2, 16)} = 8.523$, $P = 0.003$; side main effect: $F_{(1, 16)} = 1.379$, $P = 0.05$]. Post-test showed the significant increase of IRS2 mRNA level in the DBS group in the ipsilateral side to stimulation in comparison with the corresponding side in the sham group ($P < 0.05$). The IRA has prevented the elevation of IRS2 mRNA that was induced by DBS ($p < 0.05$) (Fig. 4B).

In the western blot analysis, the ratio of the phosphorylated/non-phosphorylated forms of insulin signaling components including Akt and GSK3β in the animal's hippocampus in each group were determined. No significant change was found in pAkt/Akt ratio between the groups (Fig. 4C). However, a significant change in the ratio of pGSK3β/GSK3β between the groups was found [treatment main effect: $F_{(2, 12)} = 9.935$, $P = 0.0125$]. Further post hoc analysis showed significant elevation of pGSK3β/GSK3β in the DBS group at ipsilateral side ($P < 0.05$). The DBS-induced GSK3β inactivation was significantly decreased in the IRA + DBS group ($P < 0.05$) (Fig. 4D).

3.3. EC stimulation in a delay-dependent manner improved search strategies and facilitated spatial memory formation in water maze

In the last step of our study, we were interested to know whether the EC stimulation induced neurogenesis could facilitate learning and memory processes or not. In order to ensure maximum production of new functional neurons, we stimulated animals' EC in both brain sides. Rats were trained in the water maze form 50 days after the DBS. This delay is an optimum time course for maturation and functionally integration of newborn granular cells for spatial learning (Kee et al., 2007; Kempermann et al., 2015). Latency to find the platform and distance moved to find the platform, significantly declined in all groups during training days. As shown in Fig. 5C and D, repeated measures two-way ANOVA, followed by Bonferroni's test showed that the effect of treatments was not statistically significant but the time of escape latency significantly decreased over training trials, [treatment main effect: $F_{(2, 17)} = 0.135$, $P = 0.87$; time main effect: $F_{(2, 34)} = 15.68$, $P = 0.0001$]. Same statistical results were observed for distance moved parameter [treatment main effect: $F_{(2, 17)} = 0.47$, $P = 0.063$; time main effect: $F_{(2, 34)} = 13.13$, $P = 0.0001$]. Thus, the expected effect of EC stimulation on spatial learning was not significantly detected in the training latency and distance data when analyzed statistically.

Since different strategies may be followed to find the hidden platform during training trials, analyzing the detailed qualitative aspects of

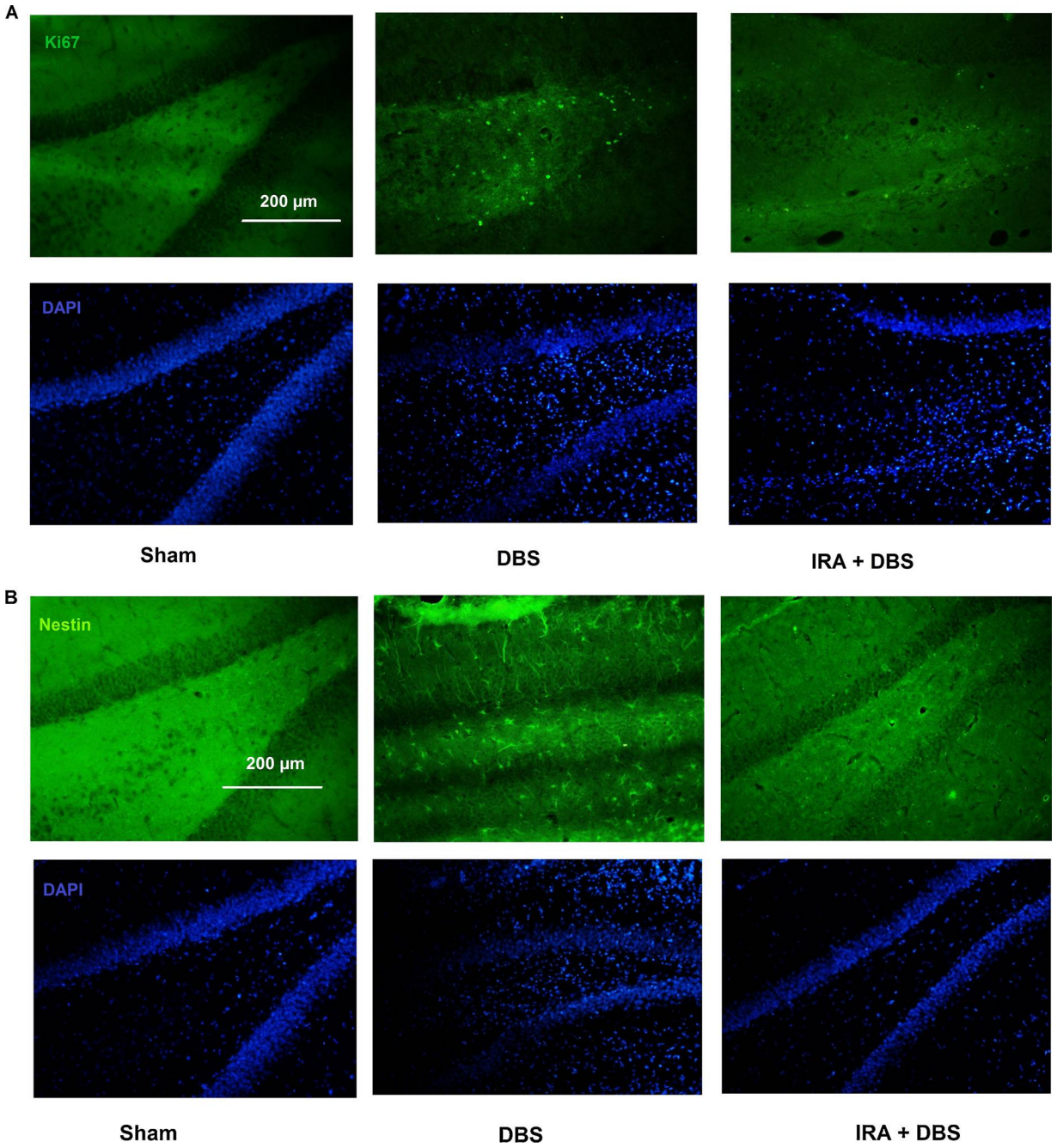

Fig. 3. The effect of unilateral entorhinal cortex stimulation on protein expression of neurogenesis markers in the dentate gyrus. Immunohistochemistry of Ki67 **(A)** and Nestin **(B)** are shown in ipsilateral hippocampus and DCX **(C)** in ipsilateral *(I)* and contralateral *(C)* hippocampus. Cell nuclei were counterstained with DAPI. Scale bar: 200 µm. DBS, deep brain stimulation; DCX, doublecortin; IRA, insulin receptor antagonist.

animals' search patterns may better clarify the spatial learning process. By using tracking data, search paths were objectively classified into eight different categories (Fig. 5B). Friedman's nonparametric analysis for each group showed following results: sham group ($\chi^2_{(7)} = 13$, $p < 0.05$), DBS group ($\chi^2_{(7)} = 16.39$, $p < 0.05$) and IRA + DBS group ($\chi^2_{(7)} = 14.66$, $p < 0.05$). As expected, on the first day of trainings, direct swim and focal search of platform accounted only for around 25 percent in sham and DBS groups, and even lower in IRA + DBS group (Fig. 5E). On the other hand, on the last day of trainings, the spatially imprecise strategies were significantly reduced and replaced by more precise behavior in all groups. As shown in Fig. 5F, at the day 3 of trainings, DBS group performed more direct swim and focal search strategies as compared to the sham group. Interestingly the percentage of direct swim and focal search were decreased in the IRA + DBS group when compared to the DBS group and even the sham group (Fig. 5G).

In probe session, one- way ANOVA showed a significant difference between groups [$F_{(2, 15)} = 4.014$, $P = 0.040$] at the time spent in target zone (Fig. 6A). Tukey's multiple comparisons test revealed that animals in the stimulation group spent significantly more time in the target zone in comparison with the sham group ($p < 0.05$), and the IRA + DBS group significantly spent less time in comparison with the DBS group ($P < 0.05$). Moreover, rats in the different groups significantly crossed the target zone differently [$F_{(2, 17)} = 3.817$, $P = 0.042$]. Tukey's post hoc analysis showed the DBS group crossed more time over the target zone in comparison with the sham group ($P < 0.05$) (Fig. 6B). Also, in the probe session, the latency to pass the platform location for the first

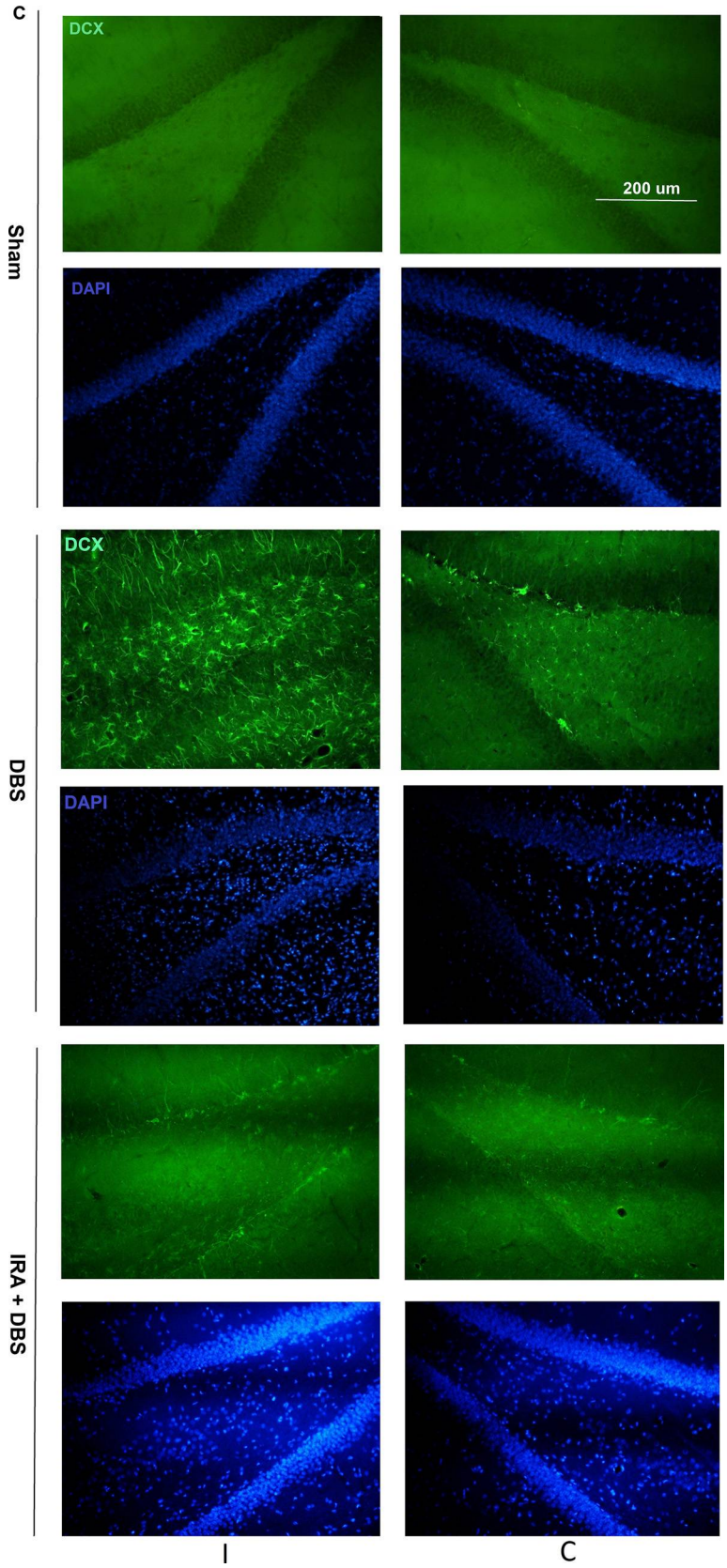

Fig. 3. (*continued*)

time was significantly different between groups [$F_{(2,\ 16)} = 14.9$, $P = 0.0002$]. Animals in the DBS group spent less time to locate the previous platform location than the sham ($P < 0.001$). However, this decrease was reversed in IRA + DBS group ($P < 0.0.5$) (Fig. 6C).Thus, in the probe day, the stimulated group showed better memory performance in comparison with the sham and the IRA + DBS group.

It is notably that measuring swim speed parameter in different experimental groups in all trials did not show significant differences (data

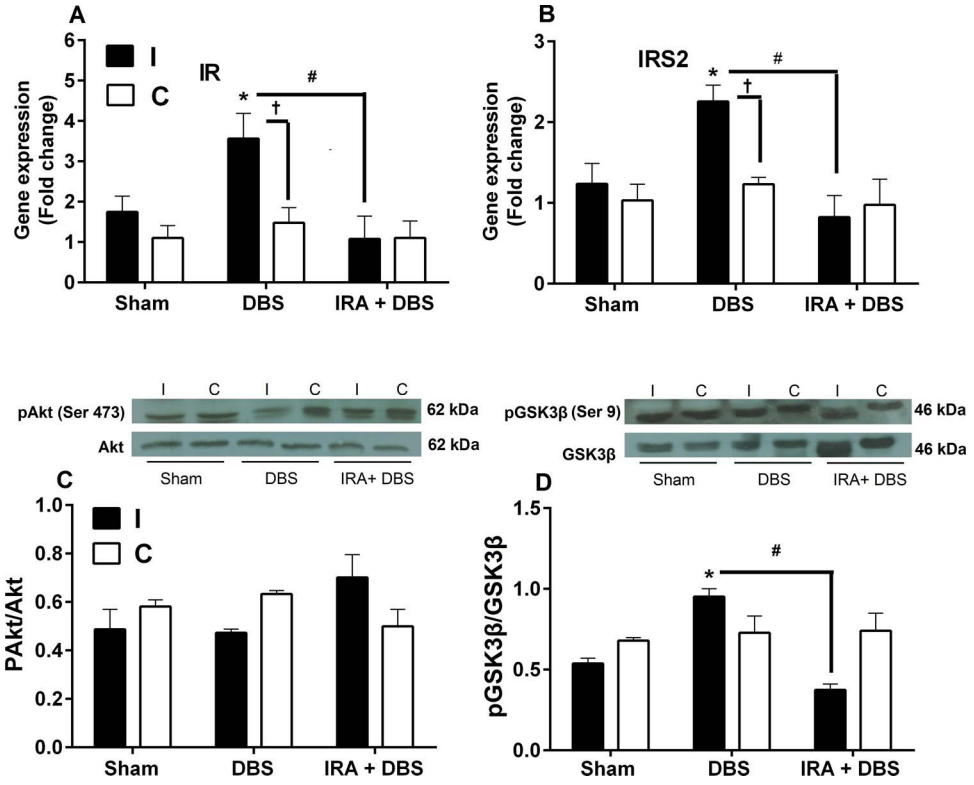

Fig. 4. The effect of unilateral entorhinal cortex stimulation on the expression of insulin signaling components in hippocampus. The qPCR data analysis of IR **(A)** and IRS2 **(B)** shows a significant increase in mRNA level of this signaling components of insulin receptor in the ipsilateral *(I)* hippocampus of the DBS group and then attenuation in the IRA + DBS group. Western blot analysis of pAkt/Akt did not show any significant change between groups **(C)**. However, western blot analysis indicated that pGSK3β/GSK3β ratio in the DBS group was significantly increased in the ipsilateral side. Administration of IRA before DBS abolished this increase in the IRA + DBS group **(D)**. The two-way ANOVA followed with Bonferroni post-test was used. Data represent Mean ± SEM. n = 3-5.$^{*}p < 0.05$ vs. corresponding sham group. $^{\#}p < 0.05$ vs. corresponding DBS group. $^{\dagger}p < 0.05$ between two sides in the DBS group. DBS, deep brain stimulation; IR, insulin receptor; IRS2, insulin receptor substrate 2; IRA, insulin receptor antagonist.

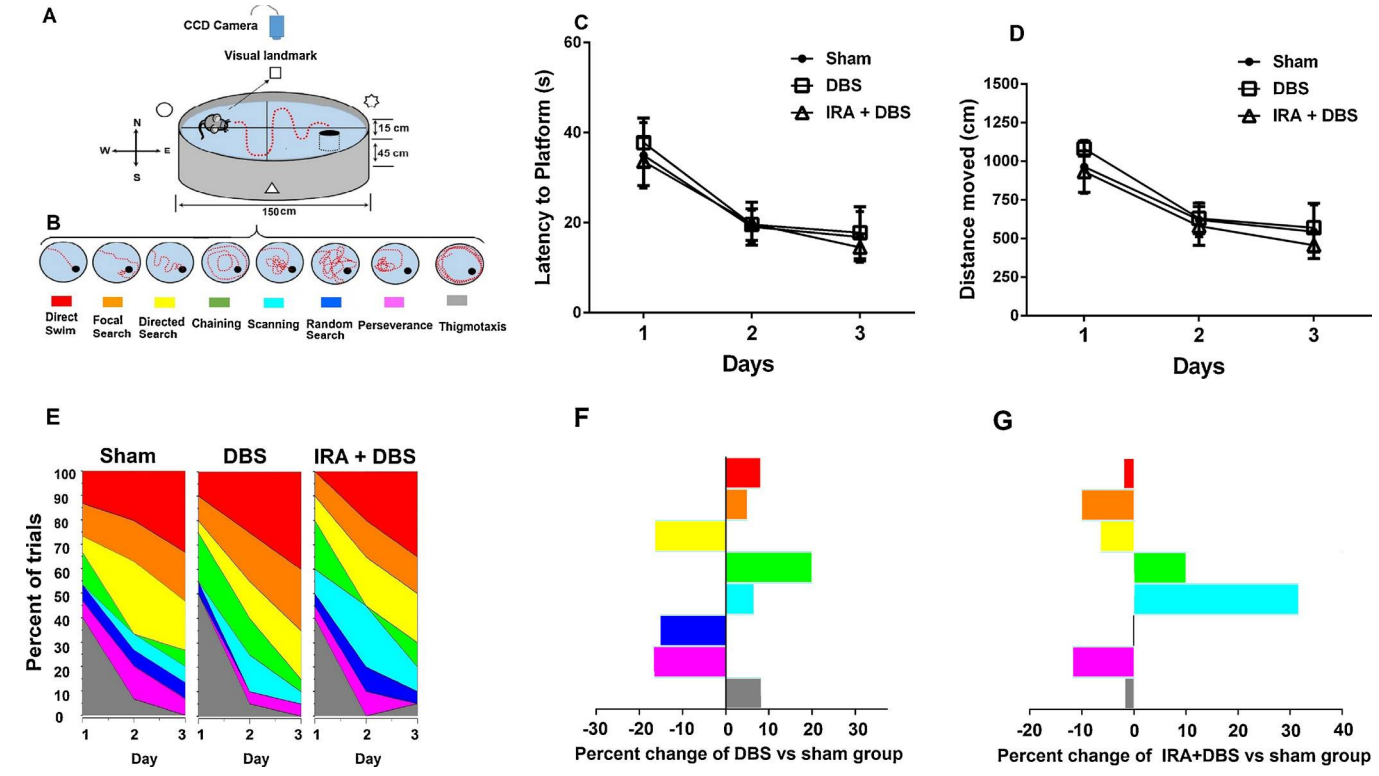

Fig. 5. Stimulation-induced enhancement of spatial learning. Water maze apparatus **(A)** and schematics of classified search strategies in the training trials **(B)** are shown. Two-way ANOVA analysis of latency to find the hidden platform **(C)** and distance moved to reach the platform **(D)** did not show significant difference between groups. Data represent Mean ± SEM. n = 6. The percentage of search strategies in each group **(E)**, and percentage difference in the number of each search strategy in DBS **(F)** and IRA + DBS **(G)** groups relative to sham group are reported across training days. DBS, deep brain stimulation; IRA, insulin receptor antagonist.

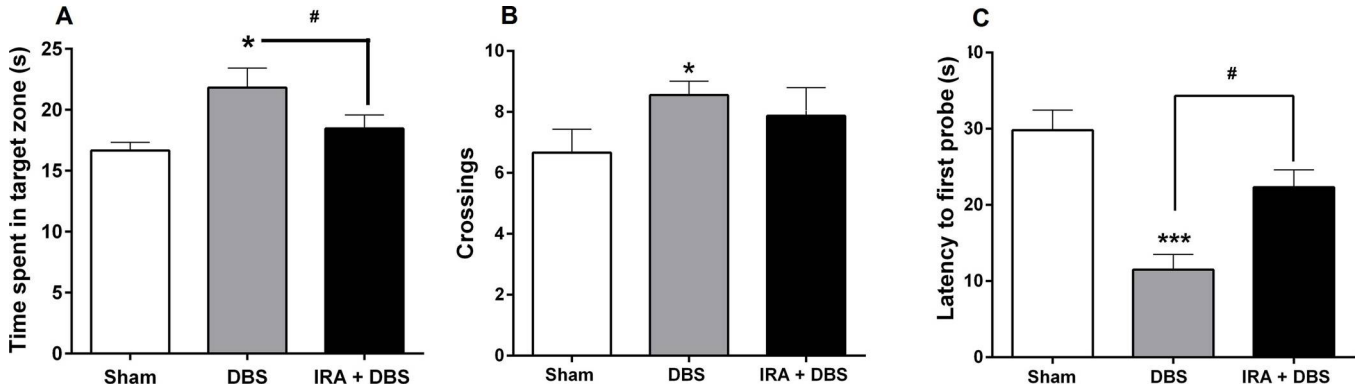

Fig. 6. In the probe trials, one-way ANOVA of the time spent in the target quadrant **(A)**, number of crossings over the previous platform location **(B)** and the latency to first cross the platform location **(C)** are reported. In the all parameters animals in the DBS group showed better memory functions in comparison to the sham and IRA + DBS groups. Data represent Mean ± SEM. n = 6. $^{*}p < 0.05$ and $^{***}p < 0.001$ vs. sham group. $^{\#}p < 0.05$ vs. DBS group. DBS, deep brain stimulation; IRA, insulin receptor antagonist.

not shown).

4. Discussion

In this study, it was observed that a single DBS treatment of the EC at adult rats induced neurogenesis in the DG region of hippocampus. Present finding is consistent with that of Stone et al. (2011) which showed that EC stimulation with the same pattern, can induce neurogenesis in the DG of adult mice (Stone et al., 2011). In another study, unilateral fimbria-fornix DBS was able to rescue spatial learning and memory and in parallel, restore hippocampal neurogenesis in a mouse model of Rett syndrome (Hao et al., 2015). Also, in a previous study, unilateral stimulation of the anteromedial thalamic nucleus in awake and unrestrained adult rats showed a significant increase of the cell proliferation markers in the ipsilateral sub-granular zone of the dentate gyrus when compared with the contralateral side and sham rats (Chamaa et al., 2016). In our study, it was interestingly observed that unilateral EC-DBS increased DCX at the level of mRNA and protein bilaterally, a phenomenon which has not been reported in studies with electrical stimulation trends. This is while this bilateral increase was not observed significantly on Nestin. This difference can be attributed to the nature of Nestin and DCX expression profile in the transition process of neural stem cells toward neuroblasts (Kempermann et al., 2015). It means, if the molecular assessments be performed at earlier time points than was done herein, day 7 post stimulus, such increase in Nestin may be also detectable. However, it can be deduced that with EC, especially layer II, stimulation in rats, the signals can reach to the contralateral DG through a homoral system and/or anatomical connections (van Groen et al., 2002) which need to be further investigated. Interestingly, Scharfman et al. have reported significant increase of neurogenesis in contralateral DG after unilateral infusion of BDNF, as a member of the neurotrophin family, into the hippocampus of adult rats without any spread of the infused BDNF to opposite hemisphere (Scharfman et al., 2005).

Remarkably, in our study in addition to subgranular region, increased neural proliferation and differentiation were seen in hilus region of DG. These ectopic hilar granular cells have been previously identified only after severe continuous seizures. However, recent studies showe that some non-pathogenic stimuli such as BDNF can also induce new born granular cells in the hilus of DG (Scharfman et al., 2005). Therefore, not only pathogenic stimuli but also some non-pathogenic factors can induce ectopic neurogenesis. Thus, granule cells that are formed in the adult brain may be misguided even when pathological condition is absent.

To assess the role of insulin signaling in neurogenesis induced by DBS, insulin receptor antagonist (IRA) was administered on the DG before EC stimulation. Most interestingly, administration of IRA attenuated both proliferation and differentiation markers. Several lines of evidence show that insulin plays a crucial role in neuronal proliferation and differentiation (Farrar et al., 2005; Roger and Fellows, 1980). There is some evidence that shows a correlation between insulin receptor signaling and neurogenesis. During cell proliferation and differentiation in the developing brain, insulin levels and the number of its receptors increase (Wozniak et al., 1993). In two detailed studies, it was shown that endogenous insulin and insulin-like growth factors and the related signaling promote proliferation and differentiation of neural stem cells derived from mouse and rat fetus (Schechter and Abboud, 2001; Vicario-Abejón et al., 2003). To make a link between EC stimulation and insulin effect on neurogenesis, it has been shown that some neurons can release insulin as a neuromodulator after the stimulation and following depolarization (Wei et al., 1990). In the present study after showing involvement of insulin receptor signaling in the EC -stimulation induced proliferation and differentiation in DG, the possible contribution of some component of insulin receptor signaling were assessed. For first step, the increased expression of IR in response to EC stimulation was observed. It has been shown that insulin receptors are present in the hippocampus in high density with partly unknown function (Marks et al., 1990). Insulin receptors in the CNS show different functional and structural properties in comparison with their peripheral counterpart. For example, IRs in the brain has been shown to respond differentially to insulin excess in comparison with those located peripherally. While peripheral IRs are downregulated in response to insulin excess, their counterparts in the brain do not show such down regulation (Ghasemi et al., 2013). There is evidence that new neural stem cells, which have been produced after neural proliferation, can express IRs in their membrane. Therefore, the observed elevation in IR mRNA can also be due to the increase in neural cell proliferation following EC-DBS and insulin release from neurons.

In the next step, to discover the downstream component of insulin receptor signaling that have been changed after EC stimulation, insulin receptors' downstream signaling pathway at mRNA and protein levels in the DBS group and in the presence of IRA were assessed. Again, markedly, the results on mRNA level showed IRS2 elevation in the stimulated group which was not seen in the group that received IRA before stimulation. In line with the present results, Schubert et al. showed that neuronal proliferation during development is severely impaired in mice lacking IRS2, showing that IRS2 signaling plays a pivotal role in neuronal proliferation during development (Schubert et al., 2003). Chirivella et al. (2017) indicated that insulin specifically promotes neurogenesis, through the activation of an IRS2/Akt/Cdk4 pathway on adult neural stem cells culture (Chirivella et al., 2017).

Moreover, to evaluate other downstream events of insulin signaling,

the Akt/GSK3β pathway assessed. In the EC-DBS group, pGSK3β/GSK3β ratio was increased and then returned to control level in animals that received insulin receptor antagonist. It is widely accepted that phosphorylation of the N-terminal serine 9 residue results in the inactivation of GSK3β (Hur and Zhou, 2010). Inhibition of GSK3β is implicated in multiple processes during neural development and in adult neurogenesis (Seira and Del Río, 2014). GSK3β inhibition has been shown to be a key regulator in signaling pathways involved in neurogenesis in neurons triggered by many extracellular molecules such as Wnt, neural growth factor (NGF), fibroblast growth factor (FGF) and sonic hedgehog (Shh) (Hur and Zhou, 2010).

Although it is widely accepted that AKT is the major mediator of serine phosphorylation and subsequent inactivation of GSK3, in our results pGSK3β/GSK3β ratio increased without any change in the Akt activity after the elevation of IR and IRS2 level in the hippocampus. Therefore, it is likely that this increase has been mediated by activation of atypical PKCs. It has been documented that following insulin binding to the receptor, in addition to Akt activation, some isoforms of PKC such as PKCζ and PKMζ can be activated. Activation of these PKC isoforms, which are called atypical PKC and highly expressed in the brain, results in GSK3β phosphorylation on Ser9 residue that finally inactivates it (Callender and Newton, 2017; Siddle, 2011).

In the current study, bilateral stimulation of the EC facilitated spatial memory formation after around 7 weeks. In the training days detailed analyses of swim paths revealed that stimulated animals were more likely to use localized/spatially precise search strategies (e.g., direct swim, focal search) and the increased frequency of these more effective strategies likely accounts for the improved spatial memory formation. In the probe test after training, stimulated rats searched more selectively as compared to non-stimulated controls. These results are consistent with two outstanding studies showing that this stimulation-induced facilitation of spatial learning is mediated by a stimulation-induced enhancement of adult neurogenesis. To confirm this hypothesis, they have shown that application of neurogenesis inhibitor, temozolomide, prevents spatial learning facilitation (Garthe et al., 2009; Stone et al., 2011). In the current study, facilitation of spatial memory formation was prevented after blocking IR by IRA, suggesting that the pro-cognitive effects of DBS are most likely mediated by insulin receptor-related mechanisms which might underlay neurogenesis. Inconsistent with the data of the current study, several studies have reported similar spatial learning deficits in animals with impaired insulin receptors signaling such as in diabetic animal models (Diegues et al., 2014) and obese animals with impaired insulin receptor signaling (Liang et al., 2015).

Collectively, the findings showed that adult neurogenesis can be one possible mechanism by which DBS exerts pro-cognitive effects. On the other hand, blocking the insulin receptor with pharmacological antagonist, demonstrated that the neurogenic and then pro-cognitive effects of EC-DBS are at least partly mediated by insulin receptor signaling. Furthermore, GSK3β inhibition might play a major role in the downstream of insulin receptor signaling in DBS induced neurogenesis.

Conflict of interest

All the authors declare that they have no conflict of interests.

Acknowledgments

This article has been extracted from the Ph.D. thesis written by Abdolaziz Ronaghi in School of Medicine, Shahid Beheshti University of Medical Sciences (Registration No: 203), funded by the Cognitive Sciences and Technologies Council of Iran (Grant No: 11P95) and Neuroscience Research Center of Shahid Beheshti University of Medical Sciences (Grant No: A-A-655).

References

Andersen, P., Morris, R., Amaral, D., O'Keefe, J., Bliss, T., 2007. The Hippocampus Book. Oxford University Press.
Boura-Halfon, S., Zick, Y., 2009. Serine Kinases of Insulin Receptor Substrate Proteins Vitam. Horm. Chapter 12. Academic Press, pp. 313–349.
Callender, J.A., Newton, A.C., 2017. Conventional protein kinase C in the brain: 40 years later. Neuronal Signal. 1https://doi.org/10.1042/NS20160005. NS20160005.
Chamaa, F., Sweidan, W., Nahas, Z., Saade, N., Abou-Kheir, W., 2016. Thalamic stimulation in awake rats induces neurogenesis in the hippocampal formation. Brain Stimul. 9, 101–108. https://doi.org/10.1016/j.brs.2015.09.006.
Chiken, S., Nambu, A., 2016. Mechanism of deep brain stimulation: inhibition, excitation, or disruption? Neuroscientist 22, 313–322. https://doi.org/10.1177/1073858415581986.
Chirivella, L., Kirstein, M., Ferrón, S.R., Domingo-Muelas, A., Durupt, F.C., Acosta-Umanzor, C., Ortega, S., 2017. Cyclin-dependent kinase 4 regulates adult neural stem cell proliferation and differentiation in response to insulin. Stem Cells 35, 2403–2416. https://doi.org/10.1002/stem.2694.
Creed, M., Pascoli, V.J., Lüscher, C., 2015. Refining deep brain stimulation to emulate optogenetic treatment of synaptic pathology. Science 347, 659–664. https://doi.org/10.1126/science.1260776.
Deuschl, G., Schade-Brittinger, C., Krack, P., Volkmann, J., Schäfer, H., Bötzel, K., Eisner, W., 2006. A randomized trial of deep-brain stimulation for Parkinson's disease. N. Engl. J. Med. 355, 896–908. https://doi.org/10.1056/NEJMoa060281.
Diegues, J.C., Pauli, J.R., Luciano, E., Almeida Leme, J.A.C., Moura, L.P., Dalia, R.A., Gomes, R.J., 2014. Spatial memory in sedentary and trained diabetic rats: molecular mechanisms. Hippocampus 24, 703–711. https://doi.org/10.1002/hipo.22261.
Encinas, J.M., Hamani, C., Lozano, A.M., Enikolopov, G., 2011. Neurogenic hippocampal targets of deep brain stimulation. J. Comp. Neurol. 519, 6–20. https://doi.org/10.1002/cne.22503.
Farrar, C., Houser, C.R., Clarke, S., 2005. Activation of the PI3K/Akt signal transduction pathway and increased levels of insulin receptor in protein repair-deficient mice. Aging Cell 4, 1–12. https://doi.org/10.1111/j.1474-9728.2004.00136.
Paxinos, G., Watson, C., 2007. The Rat Brain in Stereotaxic Coordinates.
Garthe, A., Behr, J., Kempermann, G., 2009. Adult-generated hippocampal neurons allow the flexible use of spatially precise learning strategies. PLoS One 4, e5464. https://doi.org/10.1371/journal.pone.0005464.
Ghasemi, R., Haeri, A., Dargahi, L., Mohamed, Z., Ahmadiani, A., 2013. Insulin in the brain: sources, localization and functions. Mol. Neurobiol. 47, 145–171. https://doi.org/10.1007/s12035-012-8339-9.
Gutiérrez, S., Mukdsi, J.H., Aoki, A., Torres, A.I., Soler, A.P., Orgnero, E.M., 2007. Ultrastructural immunolocalization of IGF-1 and insulin receptors in rat pituitary culture: evidence of a functional interaction between gonadotroph and lactotroph cells. Cell Tissue Res. 327, 121–132. https://doi.org/10.1007/s00441-006-0283-4.
Hao, S., Tang, B., Wu, Z., Ure, K., Sun, Y., Tao, H., Samaco, R.C., 2015. Forniceal deep brain stimulation rescues hippocampal memory in Rett syndrome mice. Nature 526, 430. https://doi.org/10.1038/nature15694.
Hur, E.-M., Zhou, F.-Q., 2010. GSK3 signalling in neural development. Nat. Rev. Neurosci. 11, 539. https://doi.org/10.1038/nrn2870.
Kee, N., Teixeira, C.M., Wang, A.H., Frankland, P.W., 2007. Preferential incorporation of adult-generated granule cells into spatial memory networks in the dentate gyrus. Nat. Neurosci. 10 (3), 355–362. https://doi.org/10.1038/nn1847.
Kempermann, G., Song, H., Gage, F.H., 2015. Neurogenesis in the adult hippocampus. Cold Spring Harb. Perspect. Biol. 7 (September (9)), a018812. https://doi.org/10.1101/cshperspect.a018812.
Kitamura, T., Saitoh, Y., Murayama, A., Sugiyama, H., Inokuchi, K., 2010. LTP induction within a narrow critical period of immature stages enhances the survival of newly generated neurons in the adult rat dentate gyrus. Mol. Brain 3, 13. https://doi.org/10.1186/1756-6606-3-13.
Kringelbach, M.L., Jenkinson, N., Owen, S.L., Aziz, T.Z., 2007. Translational principles of deep brain stimulation. Nat. Rev. Neurosci. 8, 623. https://doi.org/10.1038/nrn2196.
Laxton, A.W., Tang-Wai, D.F., McAndrews, M.P., Zumsteg, D., Wennberg, R., Keren, R., et al., 2010. A phase I trial of deep brain stimulation of memory circuits in Alzheimer's disease. Ann. Neurol. 68, 521–534. https://doi.org/10.1002/ana.22089.
Liang, L., Chen, J., Zhan, L., Lu, X., Sun, X., Sui, H., Zhang, F., 2015. Endoplasmic reticulum stress impairs insulin receptor signaling in the brains of obese rats. PLoS One 10, e0126384. https://doi.org/10.1371/journal.pone.0126384.
Marks, J.L., Porte Jr, D., Stahl, W.L., Baskin, D.G., 1990. Localization of insulin receptor mRNA in rat brain by in situ hybridization. Endocrinology 127, 3234–3236. https://doi.org/10.1210/endo-127-6-3234.
Mayberg, H.S., Lozano, A.M., Voon, V., McNeely, H.E., Seminowicz, D., Hamani, C., et al., 2005. Deep brain stimulation for treatment-resistant depression. Neuron 45, 651–660. https://doi.org/10.1016/j.neuron.2005.02.014.
Ming, G.-l., Song, H., 2005. Adult neurogenesis in the mammalian central nervous system. Annu. Rev. Neurosci. 28, 223–250. https://doi.org/10.1146/annurev.neuro.28.051804.101459.
Mishra, S.K., Singh, S., Shukla, S., Shukla, R., 2018. Intracerebroventricular streptozotocin impairs adult neurogenesis and cognitive functions via regulating neuroinflammation and insulin signaling in adult rats. Neurochem. Int. 113, 56–68. https://doi.org/10.1016/j.neuint.2017.11.012.
Noor, A., Zahid, S., 2017. Alterations in adult hippocampal neurogenesis, aberrant protein s-nitrosylation, and associated spatial memory loss in streptozotocin-induced diabetes mellitus type 2 mice. Iran. J. Basic Med. Sci. 20, 1159. https://doi.org/10.22038/IJBMS.2017.9366.

Perluigi, M., Pupo, G., Tramutola, A., Cini, C., Coccia, R., Barone, E., Di Domenico, F., 2014. Neuropathological role of PI3K/Akt/mTOR axis in Down syndrome brain. Biochim. Biophys. Acta 1842, 1144–1153. https://doi.org/10.1016/j.bbadis.2014.04.007.

Roger, L., Fellows, R., 1980. Stimulation of ornithine decarboxylase activity by insulin in developing rat brain. Endocrinology 106, 619–625. https://doi.org/10.1210/endo-106-2-619.

Scharfman, H., Goodman, J., Macleod, A., Phani, S., Antonelli, C., Croll, S., 2005. Increased neurogenesis and the ectopic granule cells after intrahippocampal BDNF infusion in adult rats. Exp. Neurol. 192, 348–356. https://doi.org/10.1016/j.expneurol.2004.11.016.

Schechter, R., Abboud, M., 2001. Neuronal synthesized insulin roles on neural differentiation within fetal rat neuron cell cultures. Dev Brain Res. 127, 41–49. https://doi.org/10.1016/S0165-3806(01)00110-9.

Schubert, M., Brazil, D.P., Burks, D.J., Kushner, J.A., Ye, J., Flint, C.L., Rio, C., 2003. Insulin receptor substrate-2 deficiency impairs brain growth and promotes tau phosphorylation. J. Neurosci. 23, 7084–7092. https://doi.org/10.1523/JNEUROSCI.23-18-07084.2003.

Seira, O., Del Río, J.A., 2014. Glycogen synthase kinase 3 beta (GSK3β) at the tip of neuronal development and regeneration. Mol. Neurobiol. 49, 931–944. https://doi.org/10.1007/s12035-013-8571-y.

Siddle, K., 2011. Signalling by insulin and IGF receptors: supporting acts and new players. J. Mol. Endocrinol. 47, R1–R10. https://doi.org/10.1530/JME-11-0022.

Stone, S.S., Teixeira, C.M., DeVito, L.M., Zaslavsky, K., Josselyn, S.A., Lozano, A.M., Frankland, P.W., 2011. Stimulation of entorhinal cortex promotes adult neurogenesis and facilitates spatial memory. J. Neurosci. 31, 13469–13484. https://doi.org/10.1523/JNEUROSCI.3100-11.2011.

van der Heide, L.P., Ramakers, G.M., Smidt, M.P., 2006. Insulin signaling in the central nervous system: learning to survive. Prog. Neurobiol. 79, 205–221. https://doi.org/10.1016/j.pneurobio.2006.06.003.

van Groen, T., Kadish, I., Wyss, J.M., 2002. Species differences in the projections from the entorhinal cortex to the hippocampus. Brain Res. Bull. 57 (3–4), 553–556. https://doi.org/10.1016/S0361-9230(01)00683-9.

Vicario-Abejón, C., Yusta-Boyo, Ma.J., Fernández-Moreno, C., de Pablo, F., 2003. Locally born olfactory bulb stem cells proliferate in response to insulin-related factors and require endogenous insulin-like growth factor-I for differentiation into neurons and glia. J. Neurosci. 23 (3), 895–906. https://doi.org/10.1523/JNEUROSCI.23-03-00895.2003.

Volkmann, J., Moro, E., Pahwa, R., 2006. Basic algorithms for the programming of deep brain stimulation in Parkinson's disease. Mov. Disord. 21 (S14). https://doi.org/10.1002/mds.20961.

Wei, L., Matsumoto, H., Rhoads, D.E., 1990. Release of immunoreactive insulin from rat brain synaptosomes under depolarizing conditions. J. Neurochem. 54, 1661–1662. https://doi.org/10.1111/j.1471-4159.1990.tb01219.

Wozniak, M., Rydzewski, B., Baker, S.P., Raizada, M.K., 1993. The cellular and physiological actions of insulin in the central nervous system. Neurochem. Int. 22, 1–10. https://doi.org/10.1016/0197-0186(93)90062.

Xu, R., Hu, Q., Ma, Q., Liu, C., Wang, G., 2014. The protease Omi regulates mitochondrial biogenesis through the GSK3β/PGC-1α pathway. Cell Death Dis. 5, e1373. https://doi.org/10.1038/cddis.2014.328.

Yu, S.W., Baek, S.H., Brennan, R.T., Bradley, C.J., Park, S.K., Lee, Y.S., et al., 2008. Autophagic death of adult hippocampal neural stem cells following insulin withdrawal. Stem Cells 26, 2602–2610. https://doi.org/10.1634/stemcells.2008-0153.

Zhao, C., Deng, W., Gage, F.H., 2008. Mechanisms and functional implications of adult neurogenesis. Cell 132, 645–660. https://doi.org/10.1016/j.cell.2008.01.033.

Zhao, W.-Q., Alkon, D.L., 2001. Role of insulin and insulin receptor in learning and memory. Mol. Cell. Endocrinol. 177, 125–134. https://doi.org/10.1016/S0303-7207(01)00455-5.

Zhao, W.-Q., Chen, H., Quon, M.J., Alkon, D.L., 2004. Insulin and the insulin receptor in experimental models of learning and memory. Eur. J. Pharmacol. 490, 71–81. https://doi.org/10.1016/j.ejphar.2004.02.045.

Zheng, R., Zhang, Z.-H., Chen, C., Chen, Y., Jia, S.-Z., Liu, Q., Song, G.-L., 2017. Selenomethionine promoted hippocampal neurogenesis via the PI3K-Akt-GSK3β-Wnt pathway in a mouse model of Alzheimer's disease. Biochem. Biophys. Res. Commun. 485, 6–15. https://doi.org/10.1016/j.bbrc.2017.01.069.

Ziegler, A.N., Levison, S.W., Wood, T.L., 2015. Insulin and IGF receptor signalling in neural-stem-cell homeostasis. Nat. Rev. Endocrinol. 11 (3), 161–170. https://doi.org/10.1038/nrendo.2014.208.